Met. Mater. Int., Vol. 18, No. 5 (2012), pp. 757~767
doi: 10.1007/s12540-012-5004-9

Interactive Effects of Aging Parameters of AA6056

Kamran Dehghani* **and Atiye Nekahi**

Department of Mining and Metallurgical Engineering, Amirkabir University of Technology (Tehran Polytechnic), Tehran, Iran

(received date: 5 August 2011 / accepted date: 8 December 2011)

The effect of thermomechanical treatment on the aging behavior of AA6056 aluminum alloy was modeled using response surface methodology (RSM). Two models were developed to predict the final yield stress (FYS) and elongation amounts as well as the optimum conditions of aging process. These were done based on the interactive effects of applied thermomechanical parameters. The optimum condition predicted by the model to attain the maximum strength was pre-aging at 80 °C for 15 h, followed by 70% cold work and subsequent final aging at 165 °C for 4 h, which resulted in the FYS of about 480 MPa. As for the elongation, the optimum condition was pre-aging at 80 °C for 15 h, followed by 30% cold work and final-aging at 165 °C for 4 h, which led to 21% elongation. To verify the suggested optimum conditions, the tests were carried out confirming the high accuracy (above 94%) of the RSM technique as well as the developed models. It is shown that the RSM can be used successfully to optimize the aging process, to determine the significance of aging parameters and to model the combination effect of process variables on the aging behavior of AA6056.

Key words: alloys, aging, mechanical properties, computer simulation, response surface methodology

1. INTRODUCTION

The 6000 series aluminum alloys are widely used in the automotive industry due to the high strength-to-weight ratio which results in saving in energy and fuel as well as in increasing safety. In addition, the Al-Mg-Si aluminum alloys can be strengthened even more through precipitation hardening [1,2] or the combination of applied thermomechanical and aging treatments. That is because the deformation either before or after the aging can enhance the mechanical properties of aluminum alloys. Therefore, many industrial applications of aluminum alloys involve cold work in conjunction with aging. The foremost of these are (i) T3 temper: solution heat treating followed by cold working and natural aging; (ii) T8 temper: solution heat treating plus cold working and artificial aging; and (iii) T9/T10 temper: the combination of artificial aging and cold working. Thus, by applying the proper thermomechanical treatments, one is able to improve significantly the final mechanical properties of aluminum alloys, including the 6000 series. As reported by Dehghani et al. [3-6], the applied thermomechanical treatments were successful in improving the mechanical properties of other aluminum alloys as well as the ultra and low carbon steels. This is especially the case during the bake-hardening process when the car bodies are subjected to baking the paint (aging) after the press forming (deformation).

As for 6000 series aluminum alloys, although there have been several studies on the effect of pre-straining and natural aging on the aging behavior of these alloys [7-9], there is almost no work regarding modeling and optimizing the effect of thermomechanical treatment (*i.e.*, pre-aging followed by cold working and final-aging) on the aging behavior of AA6056 using the new approach of response surface methodology (RSM). Among the 6000 series aluminum alloys, the AA6056 is currently used by the aerospace industry as an alternative to the AA2024 alloy due to the better intergranular corrosion resistance while having the same strength [10]. Therefore, the aim of present work was to model the effect of thermomechanical treatment (pre-aging followed by cold working and final aging) on the final yield strength and elongation of AA6056. For this purpose, a comprehensive thermomechanical treatment was designed using the new approach of RSM.

Modeling the effect of thermomechanical treatment on the ageing behavior of AA6056 involves considering many processing parameters as inputs, while the final properties after aging are offered as outputs. Therefore, from the industrial point of view, the modeling of age hardening, which requires the simulation of changes in many parameters during this

*Corresponding author: dehghani@aut.ac.ir

process, can be of significant importance. In general, a large number of variables, e.g., solution treatment (its temperature, holding time, cooling rate, etc.), pre-aging time and temperature, pre-straining path and amount, final aging time and temperature, etc. are among the variables involved in age hardening. Another concern regarding the age-hardening modeling is the nonlinear relationship among the parameters mentioned above. Using RSM to model the industrial process is a significant and practical approach that can overcome the mentioned shortcomings. Furthermore, it can be a powerful technique to predict the final properties of aged products without relying on the extensive time-consuming tests that are costly as well. Therefore, during a complex process such as aging, in which many different parameters are interacting simultaneously, a well-organized experimental design can be very advantageous in avoiding time-consuming laboratory tests and saving costs. Even in this regard, a statistical technique like RSM can be an excellent approach to optimizing the process and to investigating the effect of process parameters either individually or in combination with each other [11,12]. That is due to the capability of the RSM in generating the mathematical models as well. Once the models are developed using the RSM, they can be used to study the interactions among the process variables so as to determine their significance. Thus, the RSM has several advantages in optimizing and modeling the industrial processes that involve many variables interacting simultaneously. The RSM uses a collection of mathematical and statistical techniques to analyze and optimize the responses of multivariate systems. Therefore, the responses of a system are calculated readily and quickly without carrying out extensive experimental tests. In brief, the RSM can be used as a useful and powerful tool in designing, modeling and optimizing any industrial process.

As an example of using the RSM in optimizing industrial processes, Dehghani *et al*. [6] were able to use the RSM to successfully optimize the aging/baking behavior of AA5052. Hu *et al*. [12] and Naceur *et al*. [13] applied the RSM to optimize the parameters affecting sheet metal forming. Wang *et al*. [14] modeled the forming process using the RSM. The same approach was used by Bahloul *et al*. [11] in modeling and optimizing the bending operation. Shihani *et al*. [15] were able to model the extrusion process via the RSM. Even the residual stress in the heat affected zone during welding was optimized by RSM [16]. Ahmad *et al*. [17] used the RSM to optimize the thermal-mechanical stretching process of membranes.

Thus, the goal of the present work was to model the effect of thermomechanical treatment and to optimize the aging process of AA6056 using the RSM. The design of experiments was conducted using a central composite design (CCD). The RSM was then utilized to obtain the optimal conditions under which the best mechanical properties are achieved after aging. The RSM was also used to analyze and optimize the age-hardening process to determine the significance of each variable. The interaction effects of the process parameters were then studied using 2D and 3D contour plots. The accuracy of developed models was evaluated using P-value, T-value and R^2 amount. Moreover, the individual effects of the parameters were determined by the residual-main-effect approach.

2. EXPERIMENTAL PROCEDURES

2.1. Material and aging process

The direct chill AA6056 (Al+0.73Mg+0.97Si+0.98Cu+0.55Mn+0.43Fe in wt%) ingot was prepared with the dimensions of 100 mm×50 mm×25 mm. The ingots were homogenized at 560 °C for 6 h followed by hot rolling at 450 °C to the thickness of 8 mm. The intermediate annealing treatment was carried out at 400 °C for 2 h. Then, the specimens were cold rolled to the thickness of 4 mm. After the solution treatment at 560 °C for 1.5 h followed by water quenching, the specimens were subjected to a two-step aging process. As the first aging step, the specimens were pre-aged at 60, 70, 80, 90 and 100 °C for 5, 10, 15, 20 and 25 h. This was followed by cold rolling of 30, 40, 50, 60 and 70%. The second aging treatment, referred to as the final aging here, was carried out at 165 °C for 2, 4, 6, 8 and 10 h. Finally, all the samples were tensile tested at room temperature. The applied thermomechanical treatments described above are illustrated schematically in Fig. 1.

2.2. Designing the experiments and modeling the process

The central composite design (CCD) was used for designing the experiments required for modeling the aging process of AA6056. To do this, four parameters of pre-aging time (coded as A), pre-aging temperature (coded as B), pre-straining introduced by cold rolling (coded as C) and final aging time (coded as D) were considered as process variables. As mentioned, these variables are the most important ones affecting a complicated process such as aging.

The aim was not only to study the interaction effects of these parameters but also to determine which one of these variables exhibit a more significant effect on the mechanical properties after aging. According to the design of the experiments summarized in Table 1, five different levels for each parameter were considered. The range and the center point values regarding four independent variables are presented in

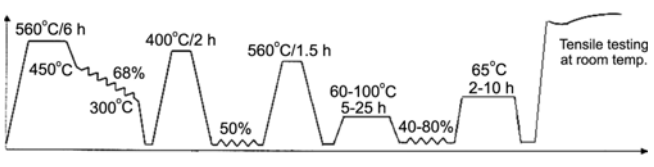

Fig. 1. The thermomechanical treatment applied in the present work.

Table 1. CCD for the studying the experimental aging variables, as well as the obtained experiment results and the predicted ones

Run No.	Experimental conditions				Results			
	Aging parameters				FYS		Elongation%	
	A: preaging time (h)	B: Preaging temp. (C)	C: prestraining (%)	D: artificial aging time (h)	Actual values (MPa)	Predicted values (MPa)	Actual values (%)	Predicted values (%)
1	-1	-1	-1	-1	407	404	18.2	17.6
2	1	-1	-1	-1	412	408	16.5	16.0
3	-1	1	-1	-1	416	412	18,6	17.6
4	1	1	-1	-1	420	418	16.8	16.3
5	-1	-1	1	-1	460	456	13.6	12.6
6	1	-1	1	-1	464	459	12	11.7
7	-1	1	1	-1	468	460	13	12.8
8	1	1	1	-1	472	466	12.5	12.0
9	-1	-1	-1	1	402	400	15.5	14.9
10	1	-1	-1	1	409	409	13.5	13.1
11	-1	1	-1	1	413	410	16	15.7
12	1	1	-1	1	425	422	14.2	14.1
13	-1	-1	1	1	450	444	11.3	11.2
14	1	-1	1	1	456	453	10	10
15	-1	1	1	1	454	451	12.7	12.1
16	1	1	1	1	467	462	11	11.1
17	-2	0	0	0	407	415	11.0	12.3
18	2	0	0	0	423	429	9.5	9.7
19	0	-2	0	0	421	427	12	12.9
20	0	2	0	0	435	444	13.4	14.1
21	0	0	-2	0	384	387	19	20.1
22	0	0	2	0	467	479	11.6	12.1
23	0	0	0	-2	438	448	14.5	16
24	0	0	0	2	435	440	12.3	12.4
25	0	0	0	0	453	455	17	16.5
26	0	0	0	0	456	455	16	16.5
27	0	0	0	0	462	455	16.3	16.5
28	0	0	0	0	448	455	15.8	16.5
29	0	0	0	0	467	455	16.8	16.5
30	0	0	0	0	453	455	16.5	16.5
31	0	0	0	0	450	455	17	16.5

Table 2. The actual and code levels of the experimental variables.

code level: variables	-2	-1	0	1	2
A: pre-aging time (h)	5	10	15	20	25
B: pre-aging temperature (°C)	60	70	80	90	100
C: pre-straining (%)	30	40	50	60	70
D: final-aging time (h)	2	4	6	8	10

Table 2. The responses were selected as the final yield stress (FYS) and elongation. The process variables were coded according to the following Eq:

$$x_i = (X_i - X_0)/\Delta X, \quad (1)$$

where x_i is the coded value of the variable X_i, X_0 is the value of any parameter at the center point and X is the step value. Based on the four variables, the responses were obtained using the quadratic Eq as:

$$Y = a_0 + \Sigma^4_{i=1} a_i X_i + \Sigma^4_{i=1} a_{ii} X_i^2 + \Sigma^3_{i=1} \Sigma^4_{j=i+1} a_{ij} X_i X_j, \quad (2)$$

where Y is the response, *i.e*., the FYS and elongation here, a_0 is a constant, while a_i, a_{ii} and a_{ij} are the coefficients, and X_i, X_j are the value of process parameters.

The models can then be used for predicting the FYS and elongation for any new thermo-mechanical condition.

2.3. Developing the contour plots

The 2D and 3D contour plots were obtained to predict the interactive effects of the aging variables, either individually or in combination with other variables, on the response surface. With the help of these plots, the combination and interaction of two variables can be studied so that their effects on the FYS and elongation responses can be optimized.

The 2D and 3D contour plots are unique approaches to

understanding clearly the interaction of the variables and to determine the optimum level of each variable in order to attain the best responses. These plots represent graphically the regression equations when each contour offers different combinations of two processing parameters to obtain the same amount of, *e.g.*, FYS, while the other variables are kept at their zero levels. The shapes of the contour plots are then used to interpret the interactions between the variables and to predict the significance of interactions. For instance, if the contour plots are circular, it means that the interactions between the variables are not very significant. By contrast, elliptical plots imply that the interactions between variables are important, *i.e.*, exhibiting strong interaction. Using these plots, one can therefore determine the optimal combination of variables for any industrial process, such as the age-hardening here. Each response plot offers an infinite number of combinations of two process variables when the other ones are kept at their respective zero levels.

3. RESULTS AND DISCUSSION

3.1. Developing the models for FYS and elongation

Based on the designed experiments, two quadratic regression models for FYS and elongation were developed as follows:

$$FYS = 455.6 + 3.62A + 4.29B + 23.04C - 2.04D - 8.32A^2 - 5.07B^2 - 5.69C^2 - 2.94D^2 + 0.69AB - 0.06AC + 1.31AD - 0.81BC + 0.56BD - 1.94DC,\ R^2 = 0.9426 \quad (3)$$

$$Elongation = 16.48 - 0.64A + 0.29B - 2C - 0.89D - 1.36A^2 - 0.75B^2 - 0.1C^2 - 0.57D^2 + 0.05AB + 0.14AC - 0.07AD + 0.02BC + 0.19BD + 0.3DC,\ R^2=0.9433 \quad (4)$$

where A, B, C and D are the coded levels of process variables.

3.2. The accuracy of the developed models

For both models, the coefficients of R^2 were obtained to evaluate the accuracy of the models. The R^2 values for FYS and elongation were obtained respectively as 0.9426 and 0.9433, which indicated more than 94% accuracy. This indicates an excellent agreement between the predicted results and those obtained experimentally. The comparison of the predicted and measured amounts is summarized in Table 1. As is obvious, there is a very good agreement between the predicted and measured values, demonstrating again the high accuracy of the developed models.

The coefficients of F-values and P-values can also be used to evaluate the accuracy of the models. With a larger F-value and a smaller P-value, the variable will be more significant. The F and P values for all variables of both the developed models are summarized in Table 3. For example, according to this table, the first and second orders of pre-aging time (A), pre-aging temperature (B) and pre-straining (C) exhibit significant effect (*i.e.*, their P-value is less than 0.05) on FYS. As for the elongation, the first and second order of pre-aging time (A) and artificial aging time (D), as well as the first order of pre-strain (C) and second order of temperature (B) present a significant effect (*i.e.*, their P-value is smaller than 0.05).

3.3. The response and contour plots

The effects of four factors as well as their interactive effects on the FYS are shown in Fig. 2. According to this figure, the effect of each variable and their interactive effects can be readily studied. Figure 2(a) depicts the two- and three-dimensional plots for the effect of pre-aging time and temperature on the FYS response, when the other two variables are held constant at their central levels, *i.e.*, for constant pre-straining (50%) and the final-aging time (6 h).

Table 3. Analyses of the results regarding the central composite design

	FYS			Elongation%		
	Regression coefficient	T-value	P-value	Regression coefficient	T-value	P-value
Constant	455.6			16.48		
A	3.62	2.22	0.041	-0.64	-3.65	0.002
B	4.29	2.63	0.018	0.29	1.66	0.117
C	23.04	14.12	0	-2	-11.37	0
D	-2.04	-1.25	0.229	-0.89	-5.07	0
A*A	-8.32	-5.56	0	-1.36	-8.46	0
B*B	-5.07	-3.39	0.004	-0.75	-4.66	0
C*C	-5.69	-3.81	0.002	-0.10	-0.62	0.541
D*D	-2.94	-1.97	0.066	-0.57	-3.57	0.003
A*B	0.69	0.34	0.735	0.05	0.23	0.819
A*C	-0.06	-0.01	0.975	0.14	0.64	0.532
A*D	1.31	0.66	0.521	-0.07	-0.35	0.732
B*C	-0.81	-0.41	0.690	0.02	0.12	0.909
B*D	0.56	0.28	0.782	0.19	0.87	0.397
C*D	-1.94	-0.97	0.347	0.30	1.39	0.183

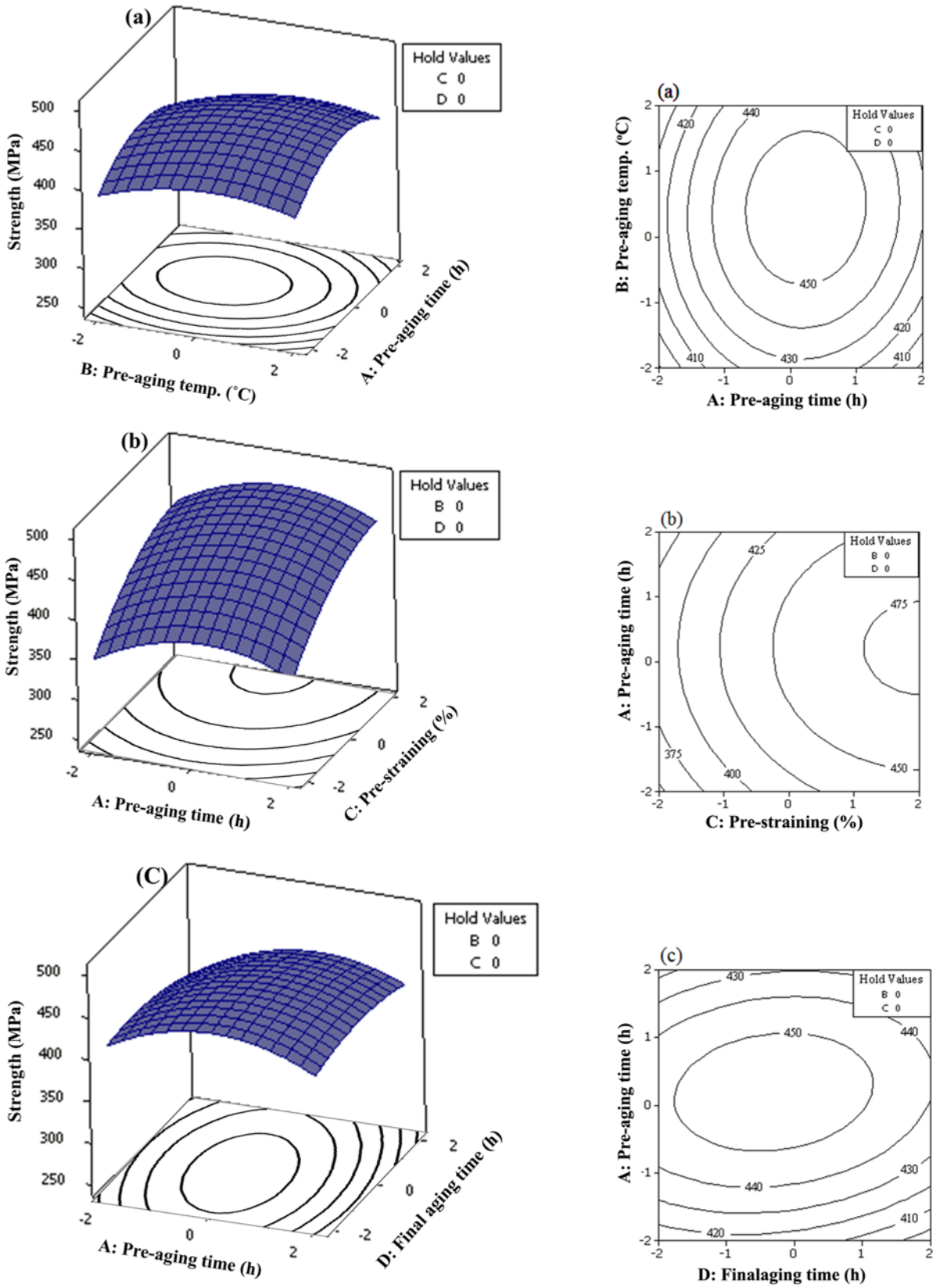

Fig. 2. 3-Dimentional plots of the FYS, for the interaction between (a): pre-aging time (A) and pre-aging temperature (B), (b): pre-straining (C) and pre-aging time (A), (c): artificial aging time (D) and pre-aging time (A), (d): artificial aging time (D) and pre-aging temperature (B), (e): artificial aging time (D) and pre-straining (C), (f) pre-straining (C) and pre-aging temperature (B).

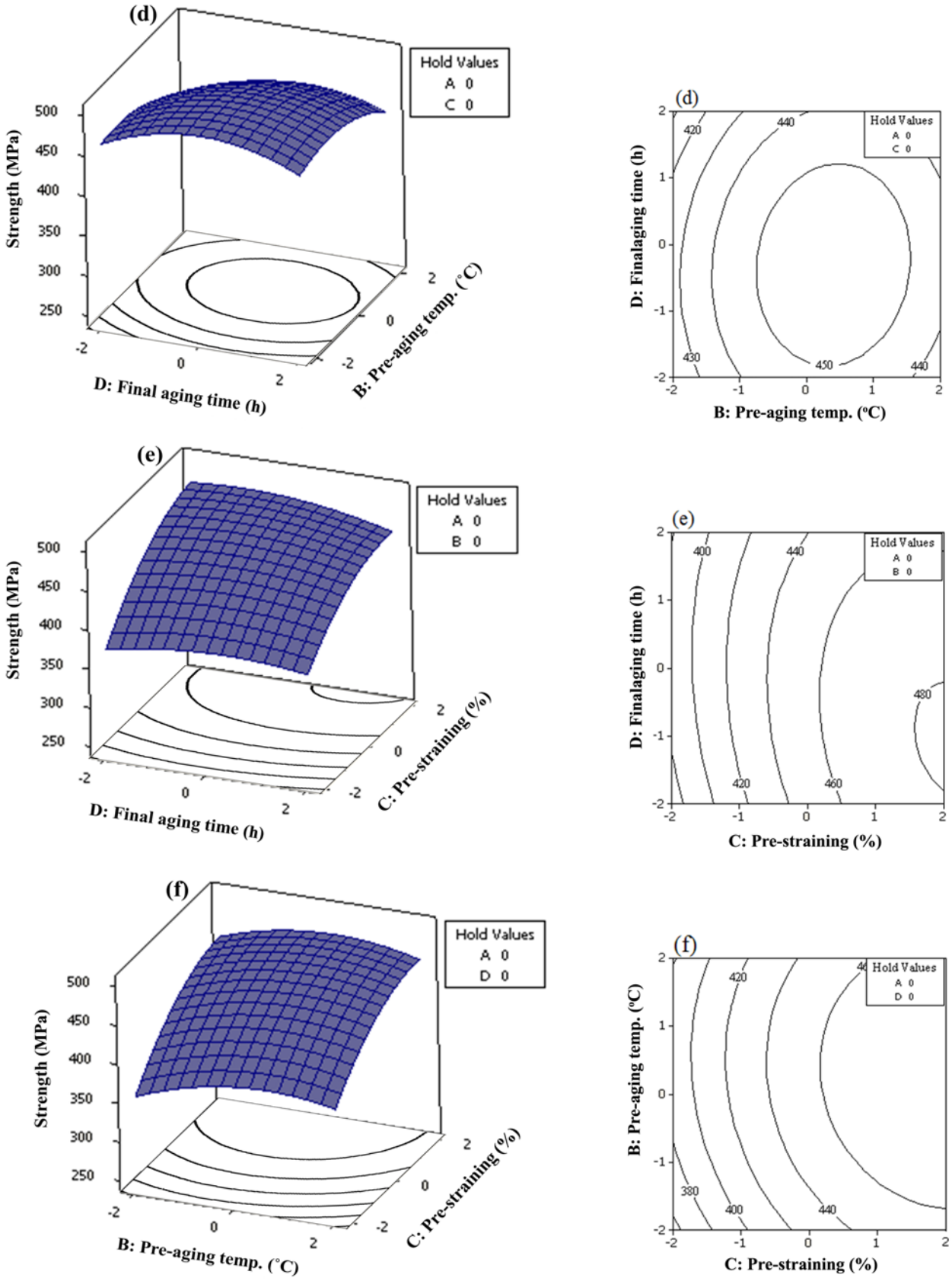

Fig. 2. (Continued)

Obviously, increasing the pre-aging time from 5 to 15 h increases the FYS, though a further increase in the pre-aging time from 15 to 25 h led to a decrease in the FYS. Furthermore, the FYS increased as the pre-aging temperature changed within 60 to 80 °C; however, the strength slightly decreased with a further increase in pre-aging temperature from 80 to 100 °C. Referring to the 2D contour plots shown on the right side of Fig. 2(a), the combination effect of pre-aging time and temperature seems to have no significant effect on the strength because the 2D contour plots are circular.

Figure 2(b) illustrates the effect of pre-aging time and pre-strain level as well as their interactive effects on the FYS, when pre-aging temperature and final-aging time are kept constant at their zero levels, *i.e*., at 80 °C and 6 h, respectively. Referring to the 2D contour plots, the interactive effects of these two variables on FYS are significant. That is because of the elliptical shape of the relative 2D contour plot. It is clear that the effect of pre-strain on the strength increment is much greater than the pre-aging time. This can be due to the significant effect of dislocations introduced by pre-straining. It is interesting that the maximum effect is obtained when the pre-aging time was 15 h. That is because there is a decrease in FYS at times higher and lower than 15 h. Therefore, the maximum FYS of 475 MPa was obtained at a 15 h pre-aging time when the pre-strain was 70%.

Figure 2(c) illustrates the combined effect of pre-aging time (A) and final-aging time (D) on the strength of AA6056 when the other two variables have their zero levels, i.e., the pre-aging temperature and pre-straining were respectively 80 °C and 50%. As presented in this figure, the strength exhibited a maximum amount of about 450 MPa at the zero levels of A (pre-aging time of 15 h) and D (final-aging time of 6 h). It is interesting that either an increase or a decrease in the zero levels of A and D resulted in a decrease in strength. The elliptical 2D contour plots presented on the right side of this figure demonstrate that the combination effects of pre-aging and final-aging times on the FYS are significant.

Figure 2(d) depicts the combined effects and pre-aging temperature (B) and final-aging time (D) on FYS when pre-aging time (A) and pre-strain amount (C) are constant, respectively, 15 h and 50%. According to this figure, the maximum strength of 475 MPa was obtained when the pre-aging temperature and final-aging time were also at their zero levels of 80 °C and 6 h, respectively. A further increase or decrease in the pre-aging temperature and final-aging time led to a decrease in FYS.

Considering Fig. 2(e), an increase in the pre-straining resulted in a significant increase in the strength of AA6056, whereas the effect of final-aging time compared to the pre-strain is less pronounced. The maximum amount of FYS (about 480 MPa) was reached with the pre-strain of 70% and final-aging time of 4 h. The same trend was observed untill the final-aging time of 4 h, and after that the strength decreased.

Finally, Fig. 2(f) presents the interaction of pre-aging temperature (B) and pre-strain (C) when pre-aging time (A) and final-aging time (D) were kept at their zero levels of 15 h and 6 h, respectively. Again, the pre-strain exhibited the strongest effect on strength. The FYS increased with a pre-aging temperature up to 80 °C, whereas a reverse effect was observed at higher temperatures.

Referring to the 3D plots, the most significant interactive effect of parameters on the FYS was the interaction between final-aging time and pre-straining (Fig. 2(e)). This resulted in the maximum FYS of about 480 MPa. The 3D plots regarding the interaction effects of variables on the elongation are shown in the Fig. 3. The same discussion can be established concerning the elongation (not mentioned for the sake of brevity).

3.4. Determining optimum conditions

During a complex process such as aging, it is essential to determine the optimum combinations of the process variables in order to attain the optimal amounts of strength and elongation. That is because the combination of strength and elongation yields the toughness that is of significant importance in terms of impact resistance required for car bodies. According to Eq. 2, the optimum condition predicted by the model to reach the maximum strength was pre-aging at 80 °C for 15 h, followed by 70% cold work and subsequent final-aging at 165 °C for 4 h. According to the developed model for FYS, aging under these conditions can result in the FYS of about 480 MPa. As for elongation, referring to Eq. 3, the optimum condition suggested by the model was pre-aging at 80 °C for 15 h followed by 30% cold work and final-aging at 165 °C for 4 h. The predicted elongation after applying this thermomechanical condition was about 21%. To validate the predicted results, two sets of experiments were carried out according to the conditions suggested by the developed models for FYS and elongation. The measured FYS and elongation obtained experimentally under the predicted conditions were about 470 MPa and 19.7%, respectively. The very good agreement between the predicted and measured amounts confirms the high accuracy of the developed models for FYS and elongation.

3.5. Mechanisms of age hardening

Although the main purposes of present work are introducing the new techniques (*i.e*., RSM including CCD, 2D and 3D contour plots) for modeling and optimizing the aging behavior of AA6056, the sequence and kinetics of precipitation during the aging of AA6056 are out of the scope of this work. Nevertheless, to evaluate the effect of aging parameters studied here, it seemed necessary to give a brief discussion of the precipitation sequence and kinetics in 6xxx aluminum series by referring to the extensive past studies;

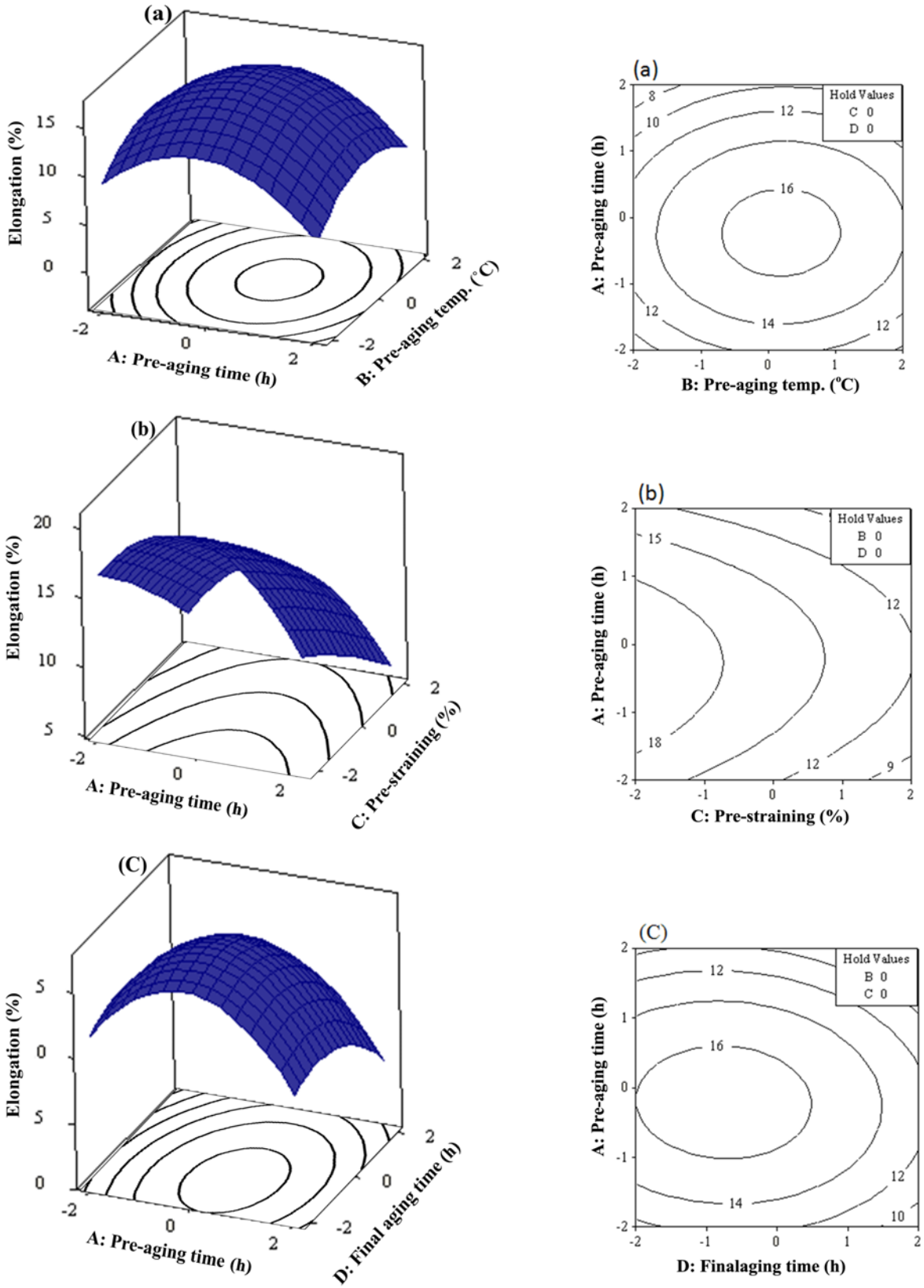

Fig. 3. 3-Dimentional plots of the elongation, for the interaction between (a): pre-aging time (A) and pre-aging temperature (B), (b): pre-straining (C) and pre-aging time (A), (c): artificial aging time (D) and pre-aging time (A), (d): artificial aging time (D) and pre-aging temperature (B), (e): artificial aging time (D) and pre-straining (C), (f) pre-straining (C) and pre-aging temperature (B).

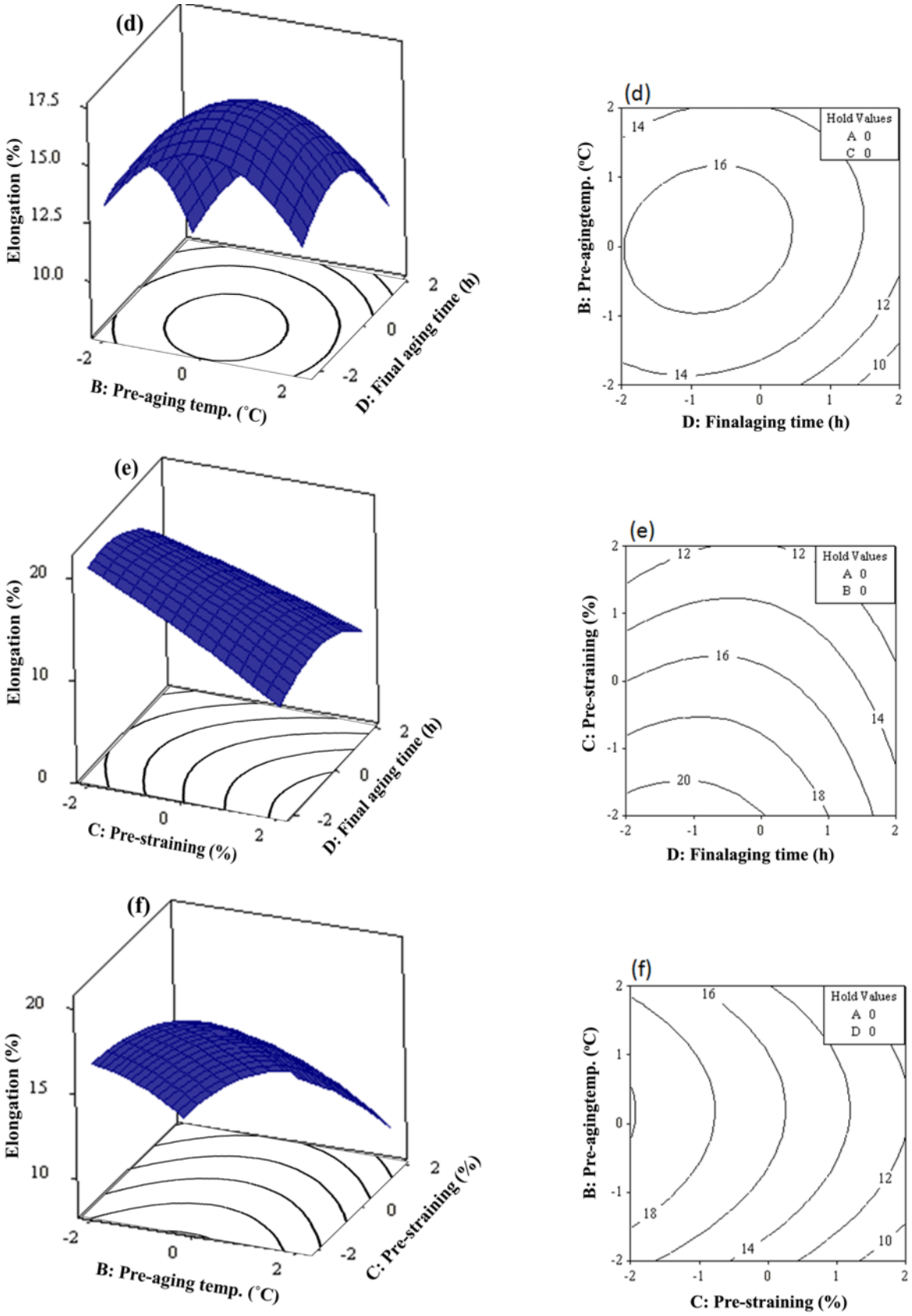

Fig. 3. (Continued)

though there are still some controversies regarding the morphology and kinetics of formed precipitates in this regard. According to the literature, the general precipitation sequence in Al-Mg-Si alloys is considered as: solid solution → GP→ $\beta'' \rightarrow \beta' \rightarrow \beta$ (Mg2Si) [18,19].

However, in case of AA6056, the situation is different because of the presence of Cu. In such a case, the metastable Q phase ($Al_5Cu_2Mg_8Si_6$) is reported to precipitate as well, making the precipitation sequence more complex. When this happens, β'' can act as a precursor for both β' and/or Q phases in Al-Mg-Si alloys containing copper. Therefore, in the presence of Cu, the precipitation sequence is proposed as follows [8,20-23]:

$$\text{Solid solution} \rightarrow \text{GP} \rightarrow \beta'' \rightarrow Q' \rightarrow Q \quad (5)$$

On studying the precipitation kinetics in AA6056 during friction stir welding, Gallais *et al*. [22] found that Q ($Al_5Cu_2Mg_8Si_6$) precipitated heterogeneously on both dispersoids and dislocations. The latter was pronounced with increasing the cold-work level. They reported that since a clear distinction between the various possible precipitates (β'' and β or Q) is possible only through the HRTEM technique, the lath-shaped precipitates were considered as Q-type whereas the needle/rod-like ones were identified as β''-type.

Generally speaking, during the early stages of final aging, the extensive inhomogeneous nucleation sites provided by dislocations (cold work) results in the formation of fine dispersed precipitates of β'' that in turn lead to an increase in the strength. As the major hardening phase in Al6056 is Q [22] rather than β'', contrary to the conventional phase transformation ($\beta'' \rightarrow \beta' \rightarrow \beta$) in Al-Mg-Si aluminum alloys, the phase transformation of $\beta'' \rightarrow Q' \rightarrow Q$ can lead to more hardening rather than softening. That is because, in the former case, the formation of metastable/stable phases β' and β is responsible for age softening rather than age hardening. In other words, in case of AA6056, whether the formed β'' transfers to other phases or not, the strengthening is satisfied.

This can justify the high strength obtained during the thermomechanical treatment applied here.

As for the effect of pre-strain, it exhibits a significant influence on the final artificial aging and in turn on the final strength. The main reason for increasing the strength can be attributed to the precipitation hardening by β''/Q formation. The same results were reported by Shen and Ou [9] in study the effect of pre-straining on the precipitation behavior of AA6022. They reported that the density of β'' precipitates was much higher due to their heterogeneous formation on the dislocations provided by pre-straining. Additionally, applying the cold work before the final aging leads to dislocation-assisted nucleation of transition phases as well as to a homogeneous and uniform distribution of dislocations. This provides extensive heterogeneous nucleation sites for precipitation when the homogeneous nucleation of precipitates is restricted.

If pre-aging is not carried out at a proper temperature (at a low temperature, *e.g*., around room temperature), the size of formed solute clusters will be significantly small, resulting in thermally unstable precipitates. If such a structure is aged at higher temperatures, the unstable phases can be readily dissolved as their critical nuclei size will be much below than that at higher temperatures. This can be regarded as the negative effect of pre-aging, *i.e*., low-temperature pre-aging such as natural aging at room temperature. As already mentioned, there could be a proper pre-aging temperature to overcome this problem. For instance, the pre-aging temperature can be increased so that the formed clusters are more stable because of a higher critical nuclei size. Such thermally stable nuclei will not only dissolve if aged at a higher temperature but rather transfer to the Q/β'', leading to an increase in the strength in a proper way.

In general, there is an optimum combination of pre-aging and subsequent cold work to take advantage of both fine-dispersed precipitates and desirable dislocation networks required before final-aging. Both can then act as heterogeneous nucleation sites to develop the fine-dispersed participates of Q-$Al_5Cu_2Mg_8Si_6$ in order to attain the optimal mechanical properties after final aging. Therefore, an optimum thermomechanical treatment (pre-aging + cold work + final aging) is required to guaranty the optimal amounts for FYS and elongation. In such a case, the increase in FYS can be achieved without ductility loss. Therefore, the main effect/role of the applied thermomechanical treatment is to provide an optimum dislocation substructure to control the volume fraction, size and distribution of the phases formed during final aging. Regarding the present work, as mentioned earlier, the optimum condition of pre-aging process was aging at 80 °C for 15 h. It is likely that under this optimal situation, the finest dispersion of stable precipitates is provided, which is required for the subsequent final aging. This is in agreement with the past work [8]. As for the final aging, the optimum condition was aging at 165 °C for 4 h. Final aging at higher temperatures or times can result in the coarsening of β''/Q precipitates or transferring of β'' to metastable β' and/or stable β leading to a decrease in FYS. Therefore, the optimum condition for aging was: (i) pre-aging at 80 °C for 15 h, (ii) 70% pre-straining, and (iii) final-aging at 165 °C for 4 h. Aging under these conditions resulted in the maximum FYS of about 480 MPa.

4. CONCLUSIONS

The response surface methodology (RSM) was successfully used to model the aging process of AA6056 and to determine the optimum conditions to achieve the optimum mechanical properties. Two models were developed to predict the effect of aging parameters (pre-aging time and tem-

perature, pre-straining and final aging time) on the responses of final yield strength and elongation.

The accuracy of the results predicted by the developed models for FYS and elongation was about 94%. The optimum conditions predicted by the models were then validated by experimental testing. The experimental results are in the good agreement with the predicted ones. The high accuracy of RSM in optimizing the aging behavior of AA6056 indicates that RSM can be an excellent tool to optimize the industrial processes.

REFERENCES

1. S. Esmaeili and D. J. Lloyd, *Acta Mater.* **53**, 5257 (2005).
2. A. K. Gupta, D. J. Lloyd, and S. A. Court, *Mat. Sci. Eng. A* **316**, 11 (2001).
3. K. Dehghani and J. J. Jonas, *Metall. Mater. Trans. A* **31**, 1375 (2000).
4. K. Dehghani and A. Shafie, *Mat. Lett.* **62**, 173 (2008).
5. A. Momeni, K. Dehghani, S. Abbasi, and M. Torkan, *MJoM* **13**, 131 (2007).
6. K. Dehghani, A. Nekahi, and M. A. Mohammad Mirzaie, *Mater. Sci. Eng. A* **527**, 7442 (2010).
7. Y. Birol, *Scripta Mater.* **52**, 1669 (2005).
8. W. F. Miao and D. E. Laughlin, *Metall. Mater. Trans. A* **31A**, 361 (2000).
9. C.-H. Shen and B.-L. Ou, *J. Chin. Inst. Eng.* **31**, 181 (2008).
10. C. Gallais, A. Simar, D. Fabregue, A. Denquin, G. Lapasset, B. De Meester, Y. Brechet, and T. Pardoen, *Metall. Mater. Trans. A* **38**, 964 (2007).
11. R. Bahloul, A. Mkaddem, P. Dal Santo, and A. Potiron, *Int. J. Mech. Sci.* **48**, 991 (2006).
12. W. Hu, L. G. Yao, and Z. Hua, *J. Mater. Process. Technol.* **197**, 77 (2008).
13. H. Naceur, S. Ben Elechi, and J. L. Batoz, *Int. Conf. on Computational Plasticity COMPLAS VIII* (Eds. E. Oñate and D. R. J. Owen) CIMNE, Barcelona, Spain (2005).
14. L. Wang, L. C. Chan, and T. C. Lee, *Int. J. Mach. Tool. Manu.* **47**, 1929 (2007).
15. N. Shihani, B. K. Kumbhar, and M. Kulshreshtha, *J. Eng. Sci. Technol.* **1**, 31 (2006).
16. A. G. Olabi, G. Casalino, K. Y. Benyounis, and A. Rotondo, *Mater. Design* **28**, 2295 (2007).
17. A. L. Ahmad, S. C. Low, S. R. Abd Shukor, and A. Ismail, *Sep. Purif. Technol.* **66**, 177 (2009).
18. I. Dutta and S. M. Allen, *J. Mater. Sci. Lett.* **10**, 323 (1991).
19. G. A. Edwards, K. Stiller, G. L. Dunlop, and M. J. Couper, *Acta Mater.* **46**, 3893 (1998).
20. D. J. Chakrabarti and D. E. Laughlin, *Prog. Mater. Sci.* **49**, 389 (2004).
21. S. Esmaeli, X. Wang, D. J. Lloyd, and W. J. Poole, *Metall. Mater. Trans. A* **34**, 751 (2003).
22. C. Gallais, A. Denquin, Y. Bréchet, and G. Lapasset, *Mater. Sci. Eng. A* **496**, 77 (2008).
23. C. A. W. Olea, L. Roldo, J. F. dos Santos, and T. R. Strohaecker, *Mater. Sci. Eng. A* **454**, 52 (2007).